Journal of Ultrafine Grained and Nanostructured Materials
https://jufgnsm.ut.ac.ir
Vol. 57, No.2, December 2024, pp. 145-157
Print ISSN: 2423-6845 Online ISSN: 2423-6837
DOI: 10.22059/jufgnsm.2024.02.05

Enhancing Conductivity in Nanocomposites: A Comprehensive Review of Silver Nanostructures and Reduced Graphene Oxide (rGO) Reinforcement Effects

Milad Zamani, Saeed Sheibani*
School of Metallurgy and Materials Engineering, College of Engineering, University of Tehran, Tehran, Iran.

Recieved: 16 October 2024 ; Accepted: 5 November 2024

**Corresponding author, E-mail:* ssheibani@ut.ac.ir

ABSTRACT

Nowadays, conductive nanocomposites are widely utilized in many applications of electronic equipment, telecommunications, the internet of things (IOT), and biosensors. Enhancing electrical properties, transparency, mechanical strength, or surface adhesion in materials for printed circuits can drive advancements in related industries. To improve the conductivity, it's significant to pay more attention to the types of electrical resistance (ER) in nanostructures such as tunneling resistance, contact resistance, and their mechanisms. Several review papers examine the synthesis processes of nanowires and how their diameter affects conductivity. Others concentrate on the mechanical properties and stability of reinforcement particles, along with efforts to synthesize rGOs and analyze their mechanical and electrical properties. However, none of these studies specifically address how morphology and synthesis impact conductivity in optoelectronic materials. This paper reviewed the various data obtained about the conductivity of single and multiple silver micro-flake, nanowires, nanoparticles, and rGO systems as 2D, 1D, and 0D nanostructures. To obtain the best conductivity by statistical methods, tried to find a mathematical relation between ER and structural parameters. Proportions of 20 wt.% for silver Micro-flakes, 20 wt.% for silver nanowires, and 5 wt.% for silver nanoparticles, respectively, may be suitable. Further, the most efficient result was obtained at the lowest aspect ratio for Ag-NWs. In general, it can be concluded that the higher the aspect ratio consequent the lower the ER. Also, probably, rGO especially without metal heteroatom can be a proper substitute for Ag micro-flakes.

Keywords: Nanostructure; Nanocomposite; Conductivity; Ag; rGO; Morphology.

1. Introduction

In recent years, nanocomposites have received much attention due to the special mechanical, electrical, and thermal properties they can have. As shown in Fig. 1., the number of published papers has increased from 103 to 2,114 between 2001 and 2023, particularly since 2010. For conductive nanocomposites, it is common to use copper (Cu), silver (Ag), carbon nanotubes (CNT), graphene, and reduced graphene oxide (rGO), both in the matrix phase and in the reinforcing phase. [1-6].

To increase the conductivity in nanocomposites, it is necessary to systematically study the methods of reducing ER. There are various theories to that explain the conduction phenomenon. Conductivity in electrolyte fluids occurs due to the movement of ions [7]. Although metal matrix composites have received much attention for application in electric and electronic industries owing to excellent thermal and electrical conductivities, in some applications it's just allowed toutilized them as reinforcement [1, 3, 8-10].

In the solid phase, the conductivity is highly dependent on the temperature of the substance, the type of atoms, the electronegativity of the atoms, their crystal structure, and the type of their interatomic bonds [11-13]. In the case of ceramics, crystal defects cause electrostatic instability, and if placed in an electric field, ions can easily pass through the mechanical energy barrier and move, or even convert into ions by transferring an additional electron to the covalent compound located coordinated them and resumption electric charge carrying electric charge transfer through them. This phenomenon also occurs in fuel cells and some oxygen sensors [14, 15]. Indeed, ions are charge carriers in ceramics. However, in metals and alloys, the situation is more complex because of the presence of metallic bonds, with electrons acting as the charge carriers. In the metal bond, there are many electrons with very low affinity to the nucleus of their atoms, which are easily transferred when placed in an electric field. Electrons must pass energy barriers to move freely. One of the parameters that resist charge transfer through electrons is grain size. Apart from pure metals, the effect of grain size on the conductivity of alloys, oxide ceramics such as Pyroxene, and nitride ceramics such as Si_3N_4 have been investigated [13, 16-18].

During the synthesis of conductive nanocomposites, various nano/micro conductive structures with different types and mechanisms are used. Conversely, multiple critical issues with these materials may cause a significant increase or decrease in conductivity. Therefore, it is necessary to check the impact of various combinations of these materials on conductivity in the optimal mode to use the least number of materials and obtain the best conductivity [8, 19-22]. For example, when moving from a material with a certain energy level to another one with a different energy level, it has to pass through an energy barrier. The phenomenon of quantum tunneling occurs when the electron tunnels through the potential barrier to pass from one energy level to a lower level when these two substances with different energy levels are at a short distance from each other while the electron goes to another energy level instead of crossing the energy barrier. This amount of energy barrier is smaller than the tunneling resistance [23].

For optoelectronic applications and nanosensors, it is important to select a material that can be synthesized at the nanoscale with high purity. For this reason, Ag is an excellent choice. The choice of synthesis method is also significant, as it influences the morphology, conductivity, and the costs. In most cases, the hydrothermal synthesis method was used to produce Ag nanowires. This method allows for the production of metal nanowires and even metal oxides at a low cost, providing the desired dimensions for various applications [21, 24-27]. Solvents in hydrothermal synthesis are cheap and available, and the crystallinity of the synthesis material can be easily controlled by changing the temperature. Metal salts are usually

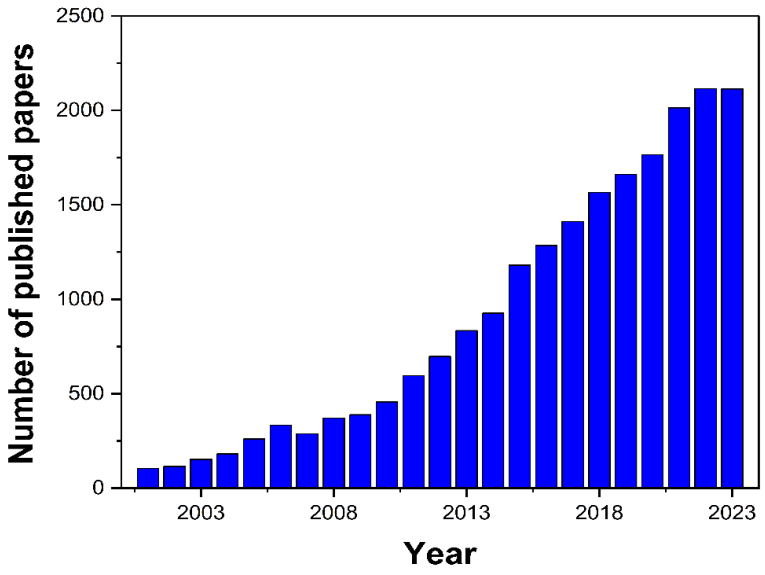

Fig. 1- Frequency of published papers from 2001 to 2023 in the nanocomposite field on the Science Direct database.

used in hydrothermal synthesis. Also, if the solvent is polar or another non-polar agent is needed during synthesis (such as ethylene glycol), the supercritical water can be used along with metal salts [28-30].

On the other hand, rGO is one of the advanced nanomaterials with a wide range of applications due to its exceptional electrical, mechanical, and thermal properties. The synthesis of rGO involves the reduction of graphene oxide (GO), which is typically achieved through various methods such as chemical reduction, thermal reduction, or electrochemical reduction. One common approach is the chemical reduction of GO using reducing agents like hydrazine (N_2H_4), and sodium borohydride ($NaBH_4$). This process leads to the restoration of sp2 carbon networks in the graphene structure, resulting in the formation of rGO with improved conductivity and reduced oxygen-containing functional groups. The synthesis of rGO is a critical step in harnessing the full potential of graphene-based materials for advanced technological applications [31, 32].

In this paper, an attempt has been made to comprehensively evaluate and compare the most important types of widely used materials in the future of optoelectronic and nanosensor industries, specifically focusing on their conductivity aspect. Furthermore, the comparison of the effect of metal heteroatoms in the structure of 2D materials and the effect of the aspect ratio of Ag nanowires on conductivity, based on the latest achievements of nanophysics has happened for the first time [33].

2. Conductivity theory

This section investigates classical, semi-classical, and modern theories of conductivity in solid-state materials. The classical model cannot explain certain phenomena at the nanoscale. The influence of temperature, crystal structure, and chemical composition on the conductivity of materials will explored [11, 23].

2.1. Classical semi-classical model

The classical theories of conductivity in metals, while successful in some respects, most notably in regard to the Wiedemann-Franz law encountered significant difficulties. These challenges have been almost completely removed by modern quantum theory [33]. There is another model known as the semi-classical Boltzmann model, which defines conductivity as a function of charge carrier density. In this model, concepts such as mean free path and relaxation time are determinants, and some of the shortcomings of the classical model are solved by this one [34]. In addition to the grain size, the grain shape is also important. Generally, the more interface between the grains and their coherence in the crystal arrangement, the more charge shall transfer per minute [11, 13].

The electron faces various resistances to transfer the charge. Tunneling resistance is explained in the quantum model of conduction [23]. The cause of this phenomenon is the wave behavior of electrons [23]. Electrons, as charge carriers, exhibit a dual wave-particle behavior when faced with a potential barrier. This is a statistical issue. That is, based on this principle, which is derived from Schrödinger's equations, a number of electrons can overcome the potential barrier if there is a small distance (less than 3 nm) between two objects, and an electron wave with a smaller amplitude enters the new object. Besides the physical distance, the type of material also influences the magnitude of the tunneling potential barrier [23].

In conductive nanocomposites, tunneling resistance is not the sole type of resistance encountered. The concept of contact resistance first appeared during the study of semiconductors. Experience shows that access to a semiconductor region through a metal contact usually exhibits a higher resistance than an ideal contact. The additional resistance that can be thought of as a series resistance in series with an ideal contact is called contact resistance [35]. The theoretical solution to semiconductor problems became possible through this mental picture. That is, it allows one to first consider the behavior of the device under the simple condition of ideal contacts and later add experimental or theoretical contact resistances that provide corrections [35]. Considering that oxidation of metal nanoparticles is inevitable; Researchers usually prefer Ag nanowires because even its oxide has good conductivity [8, 24]. While, for example, indium tin oxide, which is widely utilized, is expensive and brittle [36. 37].

2.2. Quantum model

The classical theory of conduction had shortcomings that were later solved by Sommerfeld, Houston, and Bloch with the quantum model [38]. In the classical model, the movement of electrons is considered almost free. Except that they are bound to their crystal structures. Due to their

movement being accidental and they move almost the same amount in each direction and the reverse of that direction; Rest time is considered half of the collision time [11-13]. Two mechanisms that can influence conductivity through condensation are the bending and breathing modes. Resulting in a discrete change in the metal-O bond angle and a disproportionation into expanded (metal atom sites) and contracted octahedral sites [13, 30, 33, 39]. This affects the metal-O covalence and transfers spectral weight over large energies, as observed experimentally. In the insulating phases, the metal atom sites are closer to the ionic sites. In the spin quantum number s=1 limit, the M2 sites (secondary sites) are closer to the covalent limit, with electrons in bonding orbitals forming s=0. This may be approximately ten times smaller than the large energy scales present in the system before [11]. The case investigated in this research was nickel oxide, but it can be generalized to almost all metal oxides [11, 39].

Assuming the electrons move freely, the equation of motion along the x-direction will be as follows:

$$m\, dv_x/dt = -eF \quad (1)$$

$$\int dv_x = \int (-eF/m)\, dt \quad (2)$$

$$v_d = \frac{-eF\tau}{m}\ ,\ \sigma = J/F\ ,\ J = -Ne\, v_d \quad (3)$$

$$\sigma = -Ne^2 \frac{\tau}{m} \quad (4)$$

Where F is the electric force, m is the effective mass of the electron, e is the effective charge of the electron, J is the current density, v is the velocity, and σ is the conductivity. In this way, it is concluded that conductivity has a direct relationship with the number of electrons, charge square, and an inverse relationship with the effective mass and scattering rate of electron-phonons [38]. During the completion of the conduction theory, Boltzmann's theory was proposed, in which electrons are considered semi-classically. It is assumed that an electron moves with a wave vector between scattered particles, impurities, and some other disturbances [38].

The average distance an electron travels between two scattered particles is the mean free path [7]. In this model, assuming a three-dimensional system with a spherical Fermi surface with a scanning plane, electrons are described, in other words in the semi-classical view, the chance of electrons moving in all directions is considered the same. For pure transition metals such as copper, the mean free path reaches hundreds of angstroms [13. 38]. However, this model also had some shortcomings. According to the semi-classical theory, the conductivity should decrease with an increase in temperature, as the temperature of the excitation of electrons increases. This hypothesis was supported by experimental data for 100 years, but it is violated in some cases [11]. For metals with low conductivity, this hypothesis predicts such a high scattering rate that it contradicts Heisenberg's uncertainty principle. However, the new quantum model justifies the low conductivity by examining rare cases such as nickel oxide, by examining Ni-O bond orbitals without violating the uncertainty principle. In the new relation of equal conductivity:

$$\sigma = nq^2\tau/m^* \quad (5)$$

Where n is the number of charge carriers, q is the charge of electrons, m* is the effective mass of the charge and τ is the electron-phonon scattering index. According to the principle of uncertainty, E = h/τ should be calculated. Most of the metals melt before reaching the final scattering limit, but some metals with low conductivity continue up to this temperature and become insulated by the way. The crystal structure and the degree of freedom of bonding orbitals and stretching and bending of Ni-O bonds are important in this context [11]. The crystal structure can affect the value of τ by creating interstitial spaces that are capable of swelling or breathing. In this way, with a constant density of the scattering charge, it is increased and in this way, the non-conductivity is justified [11, 40]. The longer the mean free path is, for a constant energy level, the relaxation time and electron-phonon scattering rate will be lower, and as a result, the conductivity will decrease.

2.3. Two-dimensional nanostructures model

In the case of two-dimensional nanostructures such as Graphene, two conduction modes are important. In the transversal mode where the load passes through the thickness, the following relationship is established:

$$R_s = (\sigma_b\, t)^{-1} \quad (6)$$

Where t represents the thickness and represents the bulk conductivity [8, 41]. Considering that the

conductivity of bulk graphene is not so high for multi-layer graphene [1], according to equation [12], due to their thickness of about 2 nm, high conductivity is not obtained. However, in the conduction mode, graphene has good conductivity along the length of the graphene sheet due to its two-dimensionality and sp^2 bonds [42-44]. Chemical vapor deposition (CVD) is the best method to produce graphene to achieve higher conductivity. Because in this method there are fewer defects on each page [8, 19, 38].

Theoretically, the molecular orbitals between graphene sheets and rGO are reckoned of π-π bond type. For this reason, it is at a higher energy level, and charge transfer is not done in one direction and parallel or planes, as a result, the conductivity decreases [38] for this reason, due to the van der Waals force, which increases the conductivity of graphene or rGO with metal atoms dope [38, 45-47]. In doping, it is crucial to ensure that the d-spacing between layers does not increase when incorporating more conductive metals [46]. This works like a parallel circuit for conduction along the graphene sheets by reducing the interlayer resistance [38, 47].

The importance of investigating the temperature is that in the synthesis stages of nanowires, subsequent treatments such as annealing the material are subjected to high temperatures. At high temperatures, the ER of a pure metal is approximately proportional to the absolute temperature. Weine [11] suggested that the conductivity is proportional to the mean square of the range of motion of the ions. Every metal has a certain amount of impurity, which makes the range of movement of ions around the interstitial atom not reach zero even at very low temperatures so when the temperature drops to absolute zero, the ER does not reach zero, but tends to a constant number [11].

$$R = R_T + R_0 \quad (7)$$

Where R is the total resistance, R_0 is the term depending on the temperature and R_T is the term independent of the temperature. Generally, alloying increases ER. The closer the composition ratio and the size of the atoms are, the worse the conductivity will be. As a result, we have to utilize pure Ag [33,39].

3. Conductivity of rGO

2D structures such as WSe_2, MoS_2, Fluorographene, Graphene, and rGO are of interest due to their special mechanical, optical, and electrical properties. Graphene and rGO are suitable for a wider range of applications because of their high chemical and thermal stability in three dimensions and the highest mechanical resistance and excellent electrical properties [46, 48, 49]. Therefore, a temperature of approximately 600 K is required to compromise the properties of graphene [47]. 2D structures such as rGO and graphene crystals can be formed during synthesis without impurities due to van der Waals forces [46]. However, the type of synthesis is also important. Utilizing precise methods such as CVD creates better properties.

The π-π molecular orbitals affect the electron transfer in the direction of 2D crystal

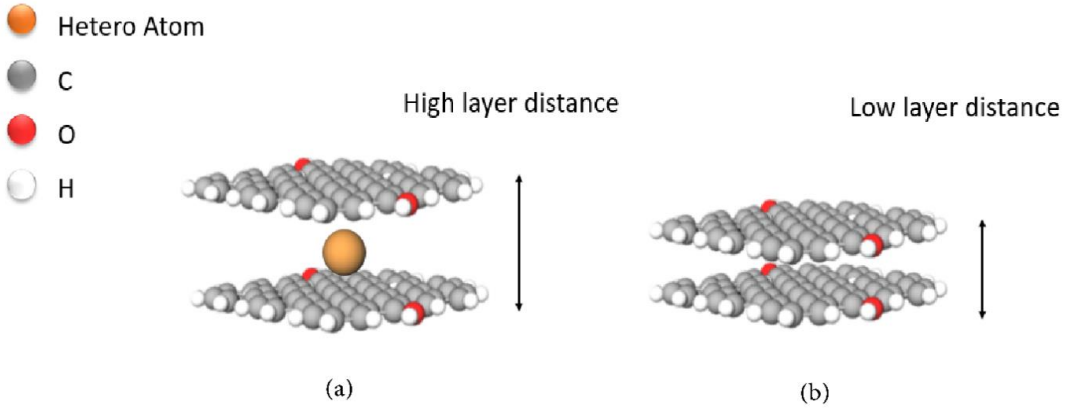

Fig. 2- (a) 3D schematic of rGO with Cu heteroatom layer distance and rGO layer distance, (b) 2D schematic of rGO crystal structure. The use of metal heteroatoms may hinder conductivity by enhancing layer distance.

accumulation. The result of Geim's research shows that a conductor with a distance between two crystals exhibits a homographic relationship [46]. As shown in Fig.2., the use of metal heteroatoms may hinder conductivity more than it enhances it, primarily due to the formation of bonding orbitals. It is essential to note that the size of the heteroatom is also crucial as it impacts the distance between the crystals. There are several ways to synthesize rGO. Such as CVD and other methods such as vacuum, evaporation and freezing the results of the conductivity test show that V> E> F have stronger accumulation structures in the order [31].

Epitaxial growth of 2D crystals such as rGO is theoretically possible. The temperature during the graphene reduction stage is essential for conductivity, thermodynamically, each reaction occurs within a specific temperature range along the reaction pathway. At a critical temperature, the reducing agent attacks a chemical bond. As per the experimental data reported by Guex et al [31], the critical temperature was 80°C [31]. The conductivity graph, based on treatment time, indicates a gradual decrease in the rate of conductivity increase from one time to the next. This phenomenon occurs because, at this temperature, the attack of the reducing agent on C-O is completed, and the attack on C=O begins [8]. The results indicate that increasing the amount of $NaBH_4$ during the treatment enhances the conductivity of rGO. As expected, temperature enhances the activity necessary for conduction. Roughness is also crucial; high roughness in the composite may lead to a short circuit [50]. The highest reported conductivity of rGO was 110 S/cm [32], while the sample doped with copper recorded 24.85 S/cm [2, 31]. However, the use of $KMnO_4$ in graphene synthesis via the Hummer method has been reported to result in reduced conductivity [51].

Because copper has a high boiling point, it is proper for high-temperature synthesis like the microwave synthesis that was done by Zeng et al. [52]. Furthermore, copper oxides like CuO and Cu_2O are also conductive, though their conductivity is lower than that of copper. They are only proper for applications like biosensors. Different concentrations of copper and various annealing temperatures were evaluated by Iskandar et al. [2], and the reduction of rGO was also done with hydrazine. Basically, among the compounds in graphene oxide, epoxy and hydroxyl groups are well regenerated and are mostly attacked by hydrazine [45, 52, 53].

There are some well-known methods for the synthesis of graphene and reduced graphene oxide (rGO) which vary in physical properties. Hydrothermal is one of the most popular methods because of cheap instruments. Nevertheless, the best results for achieving the highest possible conductivity are obtained by producing graphene via CVD and using hydrazine as a reducing agent [31, 32].

The $CuSO_4$ powder was added to NaOH to obtain the deposition of Cu $(OH)_2$. The product was then washed with deionized water and then with ethanol, then dried. Subsequently, it was dried in the oven at 60°C for 12 h [51]. Afterward, it was placed at a temperature of 700°C for 3 hours, leading to the production of CuO black powder [51]. Copper oxide produced in rGO synthesis was added to different amounts for each sample [2]. In a research study [2], copper atoms were utilized to dope reduced graphene oxide (rGO). The raw material, $CuSO_4$ powder was added to diluted water and NaOH until the deposit of Cu $(OH)_2$ was formed. Subsequently, the product was washed three times with deionized water, followed by 70 wt.% ethanol, and then dried. In this process, copper hydroxide should be placed in a furnace at 700°C for 3 h to produce CuO black powder [2,54].

In contrast, graphene produced by the Hummer method is typically subjected to lower temperatures and shorter heating times [51, 55]. In some cases, reduced graphene oxides doped with copper and copper oxide were annealed or placed in an ultrasonic bath for a while. The highest conductivity limit of 24.85 S/cm is associated with the sample annealed at 300°C for 45 minutes [56, 54].

4. Silver nanostructure

One of the factors that can affect the conductivity of nanocomposites is the structure and dimensions of Ag nanostructures. Table 1 reports previous research data about the diameter of nanowires and corresponding ER [8, 19- 21, 24, 25]. For example, according to what Cheng et al. report, the diameter was approximately 54.5 nm while the corresponding ER was equal to 18× [20].

Additionally, Table 2 reports previous research data about the length of nanowires and their corresponding ER [8, 19-21, 24, 25]. For example, according to the report by Liu et al. [21], the length was approximately 60 nm while correspond ER was equal to $2\times10^{-4}\Omega$.

Table 1- Effect of the diameter of Ag nanowires on ER

Diameter (nm)	ER ($1 \times 10^{-4}\Omega$)	Reference
54.5	18	[20]
60	2	[21]
60	10	[19]
80	5.7	[24]
200	23.3	[25]
231.4	2	[8]

Table 2- Effect of length of Ag nanowires on ER

Length (nm)	ER ($1 \times 10^{-4}\Omega$)	Reference
308	18	[20]
1500	10	[21]
10510	2	[19]
14000	5.7	[24]
32700	2	[25]

Table 3- Effect of the aspect ratio of Ag nanowires on ER

Aspect ratio	ER ($1 \times 10^{-4}\Omega$)	Reference
5.66	18	[20]
25	10	[21]
141.31	2	[19]
175	2	[24]
175	5.7	[25]

Furthermore, Table 3 reports the nanowire aspect ratio in previous efforts [19-21, 24, 25]. As Ji et al. report the average length and diameter of nanowires were 37 μm and 231 nm [25]. Also, Bellew et al. report the length of the nanowire is 1.5 μm and the diameter is 60 nm [25]. He et al. reports when the diameter of the Ag nanowires reaches 200 nm, the resistance will reach R = $2.23\times10^{-3}\Omega$/m [8].

By utilizing the data presented in Table 1, Table 2, and Table 3 and plotting the data in the form of scatter plots for each parameter, the graphs in Fig. 3 were generated. Subsequently, curve fitting was done for each graph.

Of course, these experiments were performed in different conditions with different treatments and dispersity of nanomaterials, and these factors can cause some errors in the data and conclusions. Based on the comparison made between different dimensions, it can be said that the et al. data about the relationship between the diameter of Ag nanowires and conductivity have a high yield contrary to what Huetang et al. [58] showed. No special result can be seen from the trend line of their chart. However, the length of nanowires and aspect ratio have an inverse exponential relationship with ER. Exactly the opposite of the relationship in the macroscopic dimensions, which has a direct relationship with the resistance during the length, and the resistance from the equation [58], R=ℓl/A is obtained. On a large scale, the cross-sectional area has a direct relationship with the conductivity. In bulk materials, as the length increases, the distance that charge carriers must travel, along with the number of defects and tunneling resistance they pass, also increases. Consequently, the conductivity decreases. However, in nanocomposites, due to the special processes, there are fewer structural defects and nanoscale resistance as contact or tunneling resistance. As a result, the conductivity will not decrease in length as much as in bulk materials [51].

Secondly, because the Ag nanowires are located in a polymer matrix and are not a continuous material if the length is too short, a collision between the nanowires will not occur, and the electron to transfer from one nanowire to another nanowire must overcome the resistance of the polymer matrix and the interface resistance overcome according to some efforts [8, 19-21, 24, 25]. If the length of the nanowires is short sufficient connection does not occur. Instead of moving along the desired axis, the load will move in the transverse direction. According to Fig. 4., if we consider each nanowire as a resistor, state (a) will occur when there is a longitudinal connection of nanowires, and state (b) will occur when there is no connection.

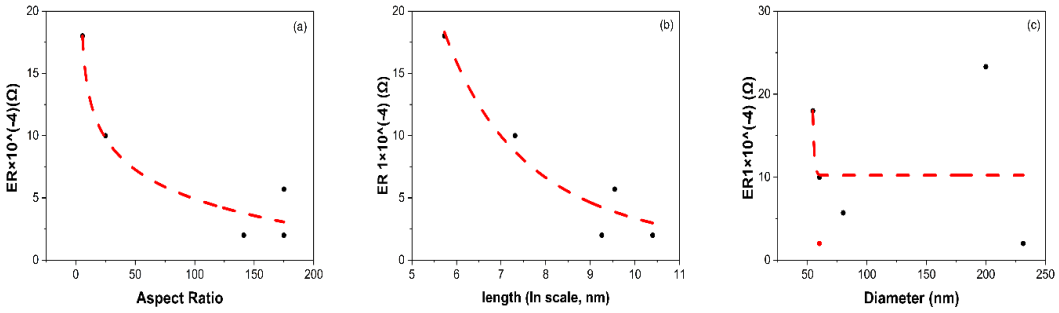

Fig. 3- Relationship between (a) resistance and aspect ratio, (b) resistance and length, and (c) resistance and diameter of Ag nanowires.

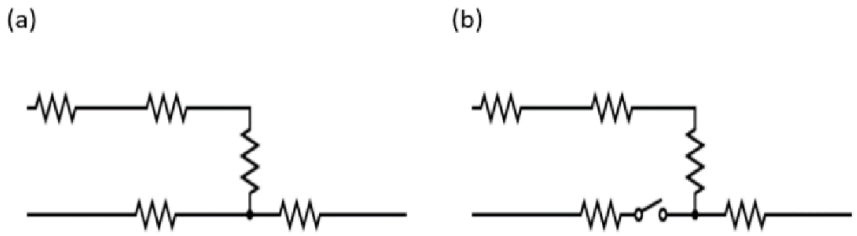

Fig. 4- Schematic of electrical circuits equivalent to situations (a) for continuous reinforcement and (b) for non-continuous.

The dimensions of nanowires are not the only structural factor affecting conductivity. When the scale of nanowires, nanospheres, or micro-flakes becomes smaller the surface energy increases. Therefore, for two samples with the same weight and composed of the same nanostructure the sample containing smaller particles will have a higher surface energy. This can greatly reduce the mono-dispersity and consequently, the conductivity will be greatly reduced [1, 20, 24].

According to the data extracted from the graph and using the curve fitting technique it seems that the relationship between the length of nanowires and ER is an exponential relationship such as below:

$$R = a + be^{(-l/c)} \quad (8)$$

Where R is the ER of the order of , l is the length of the nanowire and a, b, c are experimental constants. Also, the relationship between the aspect ratio and resistance follows the relation 9:

$$R = a - b\ln(x + c) \quad (9)$$

Where R is the ER of the order of, x is the aspect ratio of the nanowire, and a, b, c are experimental constants.

As seen in Fig. 5., Ag content does not exhibit a linear relationship with conductivity. Contrary to initial expectations, a higher number of conductive nanomaterials in the composite does not necessarily result in higher conductivity. It is almost possible to determine the range of 30 to 50% as the optimal amount of Ag content, although this may vary depending on the type of n-dimensional nanomaterial used and their dimensional ratio [1, 20, 22, 24, 59].

According to the data extracted from the mentioned papers and in the scattered form, the conductivity, expressed as weight percentage, the mass fraction of each nano/microstructure and the total Ag content, were plotted. Curve fitting was done for each of these variables and the Ag content diagram. Utilized a confidence band of 90%, the figure that is the behavior of the ER function in relation to Ag content was displayed (Figs. 5 and 6) [1, 20, 22, 24 59].

The minor ER point was masked because the great conductivity in each graph relies on the existence of other conductive nanostructures. When considering the weight fraction of nanowires in relation to the total Ag content, an intriguing observation is that varying conductivity values are observed up to approximately 70 wt.% [22]. Beyond this threshold, there is a significant increase in resistance. This phenomenon is likely attributed to interactions between the nanowires and other conductive materials. Furthermore, for nanoparticles, the optimal range of volume fraction in relation to the total Ag content is between 5 and 20 wt.% [20, 24, 46]. As shown in Fig. 6., the content of Ag nanomaterials and micro-materials has an optimal amount [1, 20, 22, 24, 59]. When the content of nanospheres exceeds 5 wt.%, resistance starts to increase due to the particles initiating the aggregation [24, 60]. Similarly, for nanowires, when the weight percentage surpasses about 20 wt.%, resistance increases once more.

However, the weight percentage of micro-flake remains relatively constant within the broad range of 20 to 45 wt.% and then rises after the ER. A certain percentage of each nanomaterial was used with different combinations of other conductive materials. So, it can be seen that for a constant number in the x-axis of each diagram, several different resistances are sometimes seen. To solve this issue, the data points that were far from the cluster were masked during interpolation (Indicated by red dots). According to other research [2, 20, 24,

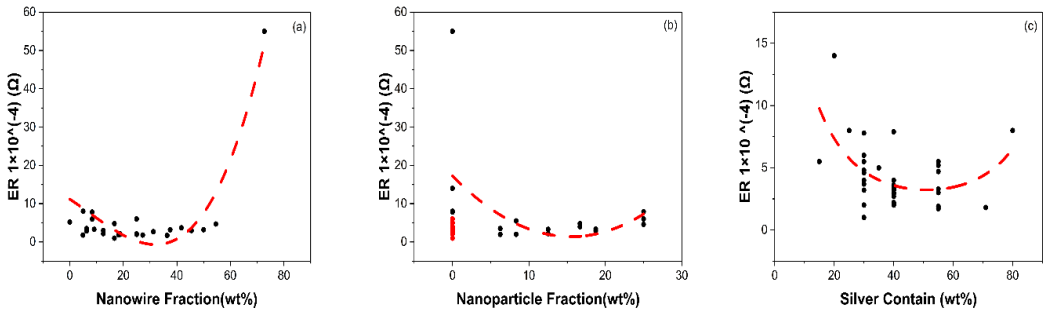

Fig. 5- Effect of and content of (a) nanowire, (b) nanoparticle, and (c) micro-flake of total Ag content on ER.

25], the cumulative effect of nanoparticles is such that if their weight percentage exceeds the optimal value, they agglomerate and no longer disperse well in the matrix, and consequently the resistance increases.

An increase in the weight percentage of nanowires from the optimal value is probably due to an increase in adhesion and an increase in the junction resistance and separation from the matrix phase. This leads to a decrease in wettability, and consequently, an increase in the tunneling resistance, which causes a decrease in conductivity [61].

In general, the data used in this section were extracted from various references. In all of these studies, both the type of matrix material and the nanomaterial synthesis method differed. Additives were also incorporated in some materials; for instance, copper nanoparticles coated with Ag were utilized to reduce the cost [62]. These cases cause parameters such as copper bulk resistance effect, and tunnel resistance difference for Ag with different polymer matrix to affect the final results, while they cannot be separated and assess their impacts, potentially leading to errors in data processing and conclusions [19-21, 24, 25, 61-64].

5. Effect of synthesis method

There are various synthesis methods for producing nanostructures. As mentioned, the purity and morphology of the nanostructure significantly affect its conductivity [2, 4]; therefore, the selection of the synthesis method is important, which will be investigated further.

Hydrothermal synthesis has weaker dimensional control and mechanical strength compared to methods such as the synthesis method in the form of anodic aluminum oxide (AAO) template although the nanowires don't need to have high strength in the construction of conductive nanocomposites [43]. In the hydrothermal synthesis of Ag nanowires, the raw material is always $AgNO_3$ and usually, ethylene glycol is used as a solvent and polyvinylpyrrolidone is used as an adhesive [19, 21, 24]. These three factors are always constant, although the molar mass of polyvinylpyrrolidone used in different formulations may vary. In some experiments, Methyl Hexahydrophthalic Anhydride (MeHHPA) was used as a curing agent [66], 2-ethyl 4-methylimidazole [64] and $FeCl_3.6H_2O$ as a catalyst, γ-2.3 epoxy propoxy as a coupling agent, and for the complete reduction of $AgNO_3$, $NaBH_4$ was used as a significant amount of ethylene glycol and volatile substances [21, 24]. Usually, the synthesized nanowires are washed with ethanol and placed in an autoclave for 24 h or more until the water and volatile substances are removed [19, 21, 24, 64].

In certain cases, post-fabrication processes like annealing or aging may be required to modify the properties of the produced nanowires [65]. Bellow et al. utilize two heat treatment methods to enhance the properties of nanowires [66- 68]. Annealing in an oxygen-free furnace and electrical activation through induction current. The first sample was annealed at 200 °C under N_2 for 2 h [25]. The second sample was annealed at 180 °C for 2 h in air. As a result, the induced current of the ER of the sample decreased from 507 to only 30 Ω in the best case. The performance of annealing in the furnace was much weaker and resulted in less resistance reduction. The reduction ratio of samples annealed with a furnace and annealed by induction current is not constant and depends on the cross-section of the nanowire. Because annealing is effective on the junction resistance. Although there are several other methods to reduce junction resistance, such as epitaxial decorating SnO_x on the tips of silver nanowires, annealing is recognized as an easy and accessible choice [69]. Overall, it can be stated

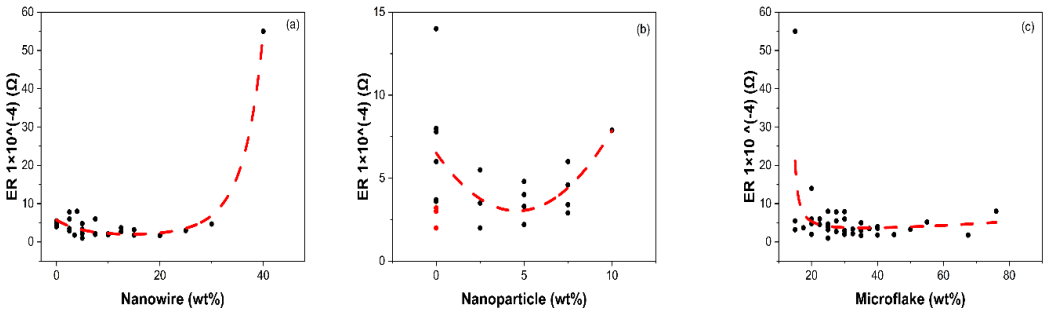

Fig. 6- Relationship between ER and content of Ag (a) nanowire, (b) nanoparticle and, (c) micro-flake.

that if the goal of annealing is to reduce ER, the induction method is significantly more effective than the furnace method [25, 54, 70].

As can be seen, annealing can affect the electrical properties of nanowires. The annealing temperature is usually around 200°C [25, 68]. Moreover, the annealing temperature is not the only critical factor. The curing temperature during cooking in the matrix and the temperature of the autoclave can also be effective. In three experiments, various synthesis temperatures were evaluated. In one instance, only a temperature of 130 °C was examined, while in the other two cases, the optimal temperature was found to be 160 °C [19, 20, 24].

In certain applications, metal nanowires serve as conductive agents in paper production. It is important to note that after mixing the nanowires with the matrix, the curing operation is performed. At temperatures above 80 °C organic coatings gradually decompose at temperatures exceeding 80 °C [19]. Therefore, it is crucial to ensure that the organic coating is not removed by crowding as much as possible. At a very high temperature, even a high weight percentage of Ag, at very high temperatures, the ER much, so it was observed that the sample containing 66 wt. % of Ag at 160 °C exhibited high ER, whereas a sample with 30 wt.% Ag at a curing temperature of 60°C showed lower ER [19, 71].

6. The challenges and open issue

Investigating the effect of temperature, time, and frequency of ultrasonic bath vibration on graphene conductivity, and the effect of time and temperature on Ag nanowires and rGO under annealing and tempering can be suitable cases for future studies. Additionally, exploring methods to reduce tunneling resistance in nanomaterials and conducting a microstructural evaluation of the interaction between nanowires and conductive nanoparticles on their electrical properties can be considered as other suitable cases.

7. Conclusion

In this paper, the effect of structural parameters on the conductivity of 1D and 2D nanostructures used in conductive nanocomposites was reviewed. The rGO can probably be a suitable substitute for Ag micro-flakes, particularly in applications where there is a greater risk of oxidation. There is a novel method for synthesis that obtain more conductive rGO than the Hummer method. To obtain more conductivity, rGO should not be doped with metal heteroatoms. Concerning Ag nanowires, it can be stated that if their weight fraction is more than 20 wt.%, it will not positively impact conductivity. This is due to the increase in junction resistance and adhesion of nanowires. The use of nanoparticles (especially nanospheres) with a weight fraction of more than 5 wt.% also causes them to agglomerate. This phenomenon, similar to nanowires, will decrease conductivity. Although using micro-flake alone is not so effective (for example, 60 wt.% Ag content of Ag micro-flake creates a conductivity equal to 35 wt.% of Ag with 10 wt.% nanowires), removing it completely or using less than 15 wt.% of it also dramatically reduces the conductivity. To calculate the optimal amount of each conductive nanomaterial, one must consider the polymer or organic matrix and the interaction between the conductive additives as important factors. To obtain better conductivity, the value of 20 wt.% for an Ag micro-flake, 20 wt.% for an Ag nanowire, and 5 wt.% for an Ag nanoparticle may be suitable. However, this optimal ratio is only calculated for conductivity and may change if we consider other application-related parameters such as wear resistance. The triple combination is more suitable and creates better conductivity with a lower weight percentage the higher the aspect ratio, the lower the ER. In short lengths, the likelihood of nanowires colliding with other conductive particles decreases, and if the diameter is increased, the probability of agglomeration increases. The formation of clusters reduces the continuity of the reinforcement phase, leading to a decrease in conductivity. By relying on this paper, researchers can gain a better vision of synthesizing the nanomaterials required for optoelectric, nanosensors and IOT applications in their future work, ultimately achieving optimal conductivity while minimizing the utilization of consumables.

Conflict of interest

The authors declare that they have no conflict of interest.

Acknowledgments

The authors express their gratitude for the assistance provided by the Iran Nanotechnology Initiative Council in supporting this paper.

References

1. Liu H, Deshmukh A, Salowitz N, Zhao J, Sobolev K. Resistivity signature of graphene-based fiber-reinforced composite subjected to mechanical loading. Frontiers in Materials. 2022; 25;9:818176.
2. Iskandar F, Abdillah OB, Stavila E, Aimon AH. The influence of copper addition on the electrical conductivity and charge transfer resistance of reduced graphene oxide (rGO). New Journal of Chemistry. 2018; 42(19):16362-71.
3. Hamedan, S. S., Abdi, M., & Sheibani, S. (2018). Comparative study on hot rolling of Cu-Cr and Cu-Cr-CNT nanocomposites. Transactions of Nonferrous Metals Society of China. 2018; 1;28(10):2044-2052.
4. Shakibhamedan S, Sheibani S, Ataie A. High performance Cu matrix nanocomposite fabricated through spark plasma sintering of Cu and Cu-coated CNT. Metals and Materials International. 2021; 27:4271-85.
5. Saleh A, Heshmati-Manesh S, Sheibani S, Ataie A. Consolidation of nano-crystalline copper powder by cold and hot pressing. Metals and Materials International. 2011; 17:749-53.
6. Harris PJ. Carbon nanotube composites. International materials reviews. 2004; 1;49(1):31-43.
7. Vargaftik NB. Handbook of thermal conductivity of liquids and gases. CRC press; 2020; 25.
8. He W, Ye C. Flexible transparent conductive films on the basis of Ag nanowires: design and applications: a review. Journal of Materials Science & Technology. 2015; 1;31(6):581-8.
9. Cao X, Shi Y, Shi W, Lu G, Huang X, Yan Q, Zhang Q, Zhang H. Preparation of novel 3D graphene networks for supercapacitor applications. small. 2011; 18;7(22):3163-8.
10. Ghorbani A, Sheibani S, Ataie A. Microstructure and mechanical properties of consolidated Cu-Cr-CNT nanocomposite prepared via powder metallurgy. Journal of Alloys and Compounds. 2018; 25;732:818-27.
11. Bardeen J. Electrical conductivity of metals. Journal of Applied Physics. 1940; 1;11(2):88-111.
12. Hagenmuller P, Van Gool W, editors. Solid electrolytes: general principles, characterization, materials, applications. Elsevier; 2013; 22.
13. Jaramillo R, Ha SD, Silevitch DM, Ramanathan S. Origins of bad-metal conductivity and the insulator–metal transition in the rare-earth nickelates. Nature Physics. 2014; 10(4):304-7.
14. Kawakami M, Goto KS, Matsuoka M. A solid electrolyte oxygen sensor for steelmaking slags of the basic oxygen converter. Metallurgical Transactions B. 1980; 11:463-9.
15. Yousefi V, Mohebbi-Kalhori D, Samimi A. Ceramic-based microbial fuel cells (MFCs): A review. International Journal of Hydrogen Energy. 2017; 19;42(3):1672-90.
16. Abbas SF, Seo SJ, Park KT, Kim BS, Kim TS. Effect of grain size on the electrical conductivity of copper–iron alloys. Journal of Alloys and Compounds. 2017; 5;720:8-16.
17. Watari K, Hirao K, Toriyama M, Ishizaki K. Effect of grain size on the thermal conductivity of Si3N4. Journal of the American Ceramic Society. 1999; 82(3):777-9.
18. Yang X, Heidelbach F. Grain size effect on the electrical conductivity of clinopyroxene. contributions to mineralogy and Petrology. 2012; 163:939-47.
19. He P, Cao J, Ding H, Liu C, Neilson J, Li Z, Kinloch IA, Derby B. Screen-printing of a highly conductive graphene ink for flexible printed electronics. ACS applied materials & interfaces. 2019; 7;11(35):32225-34.
20. Cheng Y, Zhang J, Fang C, Qiu W, Chen H, Liu H, Wei Y. Preparation of low volatile organic compounds silver paste containing ternary conductive fillers and optimization of their performances. Molecules. 2022; 19;27(22):8030.
21. Liu H, Liu J, Wang S, Jin Z, Zhu S, Ma R, Zhang W, Wang J, Li J, Song C, Zhang S. Effects of silver nano-particles and nano-wires on properties of electrically conductive adhesives. Microelectronics Reliability. 2022; 1;135:114571.
22. Peighambardoust SJ, Rikhtegar H, Mohammadzadeh Pakdel P, Mirmohseni A. Electrically conductive epoxy-based nanocomposite adhesives loaded with silver-coated copper and silver-coated reduced graphene oxide nanoparticles. Polymers for Advanced Technologies. 2019; 30(8):1996-2004.
23. Rubakov VA. Quantum mechanics in the tunneling universe. Physics Letters B. 1984; 29;148(4-5):280-6.
24. Ji YH, Liu Y, Huang GW, Shen XJ, Xiao HM, Fu SY. Ternary Ag/epoxy adhesive with excellent overall performance. ACS applied materials & interfaces. 2015; 22;7(15):8041-52.
25. Bellew AT, Manning HG, Gomes da Rocha C, Ferreira MS, Boland JJ. Resistance of single Ag nanowire junctions and their role in the conductivity of nanowire networks. ACS nano. 2015; 24;9(11):11422-9.
26. Yang Z, Qian H, Chen H, Anker JN. One-pot hydrothermal synthesis of silver nanowires via citrate reduction. Journal of colloid and interface science. 2010; 15;352(2):285-91.
27. Zhang Y, Li G, Jin Y, Zhang Y, Zhang J, Zhang L. Hydrothermal synthesis and photoluminescence of TiO2 nanowires. Chemical Physics Letters. 2002; 365(3-4):300-4.
28. Aksomaityte G, Poliakoff M, Lester E. The production and formulation of silver nanoparticles using continuous hydrothermal synthesis. Chemical engineering science. 2013; 14;85:2-10.
29. Zou J, Xu Y, Hou B, Wu D, Sun Y. Controlled growth of silver nanoparticles in a hydrothermal process. China Particuology. 2007; 1;5(3):206-12.
30. Adschiri T, Kanazawa K, Arai K. Rapid and continuous hydrothermal crystallization of metal oxide particles in supercritical water. Journal of the American Ceramic Society. 1992; 75(4):1019-22.
31. Guex LG, Sacchi B, Peuvot KF, Andersson RL, Pourrahimi AM, Ström V, Farris S, Olsson RT. Experimental review: chemical reduction of graphene oxide (GO) to reduced graphene oxide (rGO) by aqueous chemistry. Nanoscale. 2017; 9(27):9562-71.
32. Chen J, Bi H, Sun S, Tang Y, Zhao W, Lin T, Wan D, Huang F, Zhou X, Xie X, Jiang M. Highly conductive and flexible paper of 1D silver-nanowire-doped graphene. ACS applied materials & interfaces. 2013; 27;5(4):1408-13.
33. Bardeen J. Electrical conductivity of metals. Journal of Applied Physics. 1940; 1;11(2):88-111.
34. Stauber T, Peres NM, Guinea F. Electronic transport in graphene: A semiclassical approach including midgap states. Physical Review B—Condensed Matter and Materials Physics. 2007; 15;76(20):205423.
35. Berger HH. Contact resistance and contact resistivity. Journal of the Electrochemical Society. 1972; 1;119(4):507.
36. Szkutnik PD, Roussel H, Lahootun V, Mescot X, Weiss F, Jiménez C. Study of the functional properties of ITO grown by metalorganic chemical vapor deposition from different indium and tin precursors. Journal of alloys and compounds. 2014; 5;603:268-73.
37. Wu H, Hu L, Carney T, Ruan Z, Kong D, Yu Z, Yao Y, Cha JJ, Zhu J, Fan S, Cui Y. Low reflectivity and high flexibility of tin-doped indium oxide nanofiber transparent electrodes. Journal of the American Chemical Society. 2011; 12;133(1):27-9.
38. Malik MTU, Sarker A, Rahat SSM, Shuchi SB. Performance enhancement of graphene/GO/rGO based supercapacitors: A comparative review. Materials Today Communications. 2021; 1;28:102685.
39. Bridgman PW. The resistance of nineteen metals to 30,000 kg/cm2. InPapers 94-121 1964; 31 (pp. 3203-3254). Harvard University Press.
40. Hofman GL. Crystal structure stability and fission gas swelling in intermetallic uranium compounds. Journal of Nuclear Materials. 1986; 1;140(3):256-63.
41. Haacke G. New figure of merit for transparent conductors. Journal of Applied physics. 1976; 1;47(9):4086-9.
42. Alemour B, Yaacob MH, Lim HN, Hassan MR. Review of Electrical Properties of Graphene Conductive Composites. International Journal of Nanoelectronics & Materials. 2018; 1;11(4).
43. Bøggild P, Mackenzie DM, Whelan PR, Petersen DH, Buron

JD, Zurutuza A, Gallop J, Hao L, Jepsen PU. Mapping the electrical properties of large-area graphene. 2D Materials. 2017; 6;4(4):042003.
44. Ke Q, Wang J. Graphene-based materials for supercapacitor electrodes–A review. Journal of Materiomics. 2016; 1;2(1):37-54.
45. Gao W, Alemany LB, Ci L, Ajayan PM. New insights into the structure and reduction of graphite oxide. Nature chemistry. 2009; 1(5):403-8.
46. Geim AK, Grigorieva IV. Van der Waals heterostructures. Nature. 2013; 25;499(7459):419-25.
47. Liu L, Ryu S, Tomasik MR, Stolyarova E, Jung N, Hybertsen MS, Steigerwald ML, Brus LE, Flynn GW. Graphene oxidation: thickness-dependent etching and strong chemical doping. Nano letters. 2008; 9;8(7):1965-70.
48. Batista BL, Fuentes GT, Lobato AK, editors. The Role of Gasotransmitters in the Amelioration of Arsenic Toxicity in Plants: Biology and Biotechnology. Elsevier; 2023 ;27.
49. Batool S, Idrees M, Han ST, Roy VA, Zhou Y. Electrical contacts with 2D materials: current developments and future prospects. Small. 2023; 19(12):2206550.
50. Zeng XY, Zhang QK, Yu RM, Lu CZ. A new transparent conductor: silver nanowire film buried at the surface of a transparent polymer. Advanced materials. 2010; 3;40(22):4484-8.
51. Husnah M, Fakhri HA, Rohman F, Aimon AH, Iskandar F. A modified Marcano method for improving electrical properties of reduced graphene oxide (rGO). Materials Research Express. 2017; 5;4(6):064001.
52. Zeng J, Bejtka K, Di Martino G, Sacco A, Castellino M, Re Fiorentin M, Risplendi F, Farkhondehfal MA, Hernández S, Cicero G, Pirri CF. Microwave-Assisted Synthesis of Copper-Based Electrocatalysts for Converting Carbon Dioxide to Tunable Syngas. ChemElectroChem. 2020; 2;7(1):229-38.
53. Pytlakowska K, Kocot K, Pilch M, Zubko M. Ultrasound-assisted dispersive micro-solid phase extraction using molybdenum disulfide supported on reduced graphene oxide for energy dispersive X-ray fluorescence spectrometric determination of chromium species in water. Microchimica Acta. 2020; 187:1-0.
54. Szostak R, Morais A, Carminati SA, Costa SV, Marchezi PE, Nogueira AF. Application of graphene and graphene derivatives/oxide nanomaterials for solar cells. InThe future of semiconductor oxides in next-generation solar cells 2018; 1 (pp. 395-437). Elsevier.
55. Wang L, Xu L, Sun C, Qian Y. A general route for the convenient synthesis of crystalline hexagonal boron nitride micromesh at mild temperature. Journal of Materials Chemistry. 2009; 19(14):1989-94.
56. Hsieh CT, Lin WH, Chen YF, Tzou DY, Chen PQ, Juang RS. Microwave synthesis of copper catalysts onto reduced graphene oxide sheets for non-enzymatic glucose oxidation. Journal of the Taiwan Institute of Chemical Engineers. 2017; 1;71:77-83.
57. Wang B, He J, Liu F, Ding L. Rapid synthesis of Cu2O/CuO/rGO with enhanced sensitivity for ascorbic acid biosensing. Journal of Alloys and Compounds. 2017; 5;693:902-8.
58. Huang GW, Xiao HM, Fu SY. based silver-nanowire electronic circuits with outstanding electrical conductivity and extreme bending stability. Nanoscale. 2014; 6(15):8495-502.
59. Ding S, Ying J, Chen F, Fu L, Lv Y, Zhao S, Ji G. Highly stretchable conductors comprising composites of silver nanowires and silver flakes. Journal of Nanoparticle Research. 2021; 23(4):111.
60. Solopan SO, V'yunov OI, Belous AG, Polek TI, Tovstolytkin AI. Effect of nanoparticles agglomeration on electrical properties of La1− xAxMnO3 (A= Sr, Ba) nanopowder and ceramic solid solutions. Solid state sciences. 2012; 1;14(4):501-5.
61. Gunnarsson O, Calandra M, Han JE. Colloquium: Saturation of electrical resistivity. Reviews of Modern Physics. 2003; 3;75(4):1085.
62. Hu L, Kim HS, Lee JY, Peumans P, Cui Y. Scalable coating and properties of transparent, flexible, silver nanowire electrodes. ACS nano. 2010; 25;4(5):2955-63.
63. Wu HP, Liu JF, Wu XJ, Ge MY, Wang YW, Zhang GQ, Jiang JZ. High conductivity of isotropic conductive adhesives filled with silver nanowires. International journal of adhesion and adhesives. 2006; 1;26(8):617-21.
64. Hui X, Nana X, Yuzhen Z, Yuehui W. Effect of silver nanowires on the resistivity of electronically conductive adhesives. Rare Metal Materials and Engineering. 2016; 1;45(10):2503-8.
65. Nasikhudin N, Yusril A, Istiqomah I, Hari R, Markus D, and Herlin P. Silver Nanowires (AgNWs) Post-Treatment Effect in Application of Flexible Transparent and Conductive Electrodes: A Mini Review. Materials Science Forum. 2024; vol. 1118, pp. 47-57. Trans Tech Publications Ltd.
66. Sarkar J, Khan GG, Basumallick A. Nanowires: properties, applications and synthesis via porous anodic aluminium oxide template. Bulletin of Materials Science. 2007; 30:271-90.
67. Li XS, Xiang XZ, Wang L, Bai XJ. Conductivity and mechanical properties of conductive adhesive with silver nanowires. Rare Metals. 2018; 37:191-5.
68. Bellew AT, Manning HG, Gomes da Rocha C, Ferreira MS, Boland JJ. Resistance of single Ag nanowire junctions and their role in the conductivity of nanowire networks. ACS nano. 2015 24;9(11):11422-9.
69. Vogl LM, Kalancha V, Schweizer P, Denninger P, Wu M, Brabec C, Forberich K, Spiecker E. Influence of tin oxide decoration on the junction conductivity of silver nanowires. Nanotechnology. 2023 13;34(17):175706.
70. Kelly AG, Hallam T, Backes C, Harvey A, Esmaeily AS, Godwin I, Coelho J, Nicolosi V, Lauth J, Kulkarni A, Kinge S. All-printed thin-film transistors from networks of liquid-exfoliated nanosheets. Science. 2017; 7;356(6333):69-73.
71. Preston C, Fang Z, Murray J, Zhu H, Dai J, Munday JN, Hu L. Silver nanowire transparent conducting paper-based electrode with high optical haze. Journal of Materials Chemistry C. 2014;2(7):1248-54.